



ARTICLE

Fine-tuning the antimicrobial activity of β -hairpin peptides with fluorinated amino acids

Suvrat Chowdhary¹  | Tim Pelzer¹ | Mareike Saathoff² | Elisa Quaas³ | Johanna Pendl⁴ | Marcus Fulde^{2,5} | Beate Kokschi¹ 

¹Institute of Chemistry and Biochemistry, Freie Universität Berlin, Berlin, Germany

²Institute of Microbiology and Epizootics, Centre of Infection Medicine, Freie Universität Berlin, Berlin, Germany

³Institute of Chemistry and Biochemistry, Core Facility SupraFAB, Freie Universität Berlin, Berlin, Germany

⁴Institute of Veterinary Anatomy, Freie Universität Berlin, Berlin, Germany

⁵Veterinary Centre for Resistance Research (TZR), Freie Universität Berlin, Berlin, Germany

Correspondence

Beate Kokschi, Institute of Chemistry and Biochemistry, Freie Universität Berlin, Arnimallee 20, 14195 Berlin, Germany. Email: beate.kokschi@fu-berlin.de

Funding information

Deutsche Forschungsgemeinschaft, Grant/Award Number: CRC-1349"Fluorine-SpecificInteractions"/387284271

Abstract

Antimicrobial peptides (AMPs) possess bactericidal activity against a variety of pathogens depending on an overall balance of positively charged and hydrophobic residues. Selective fluorination of peptides serves to fine-tune the intrinsic hydrophobicity and that could improve AMP bioactivity without affecting the sequence length. Only a few studies have focused on the impact of this unique element on antimicrobial potency and came to somewhat contractionary results. Moreover, the influence of fluorinated amino acids on peptide proteolysis is yet not fully understood. In this work, we tackle the link between side chain fluorination and both antimicrobial activity and proteolytic stability for two series of amphiphilic β -hairpin peptides. In particular, a synergy between antimicrobial activity and peptide hydrophobicity was determined. All peptides were found to be barely hemolytic and non-toxic. Most surprisingly, the fluorinated peptides were susceptible to enzymatic degradation. Hence, the distinctive properties of these polyfluorinated AMPs will serve for the future design of peptide-based drugs.

KEYWORDS

antimicrobial peptides, fluorinated antibiotics, fluorinated biomaterials, peptide digestion, polyfluorinated oligopeptides

1 | INTRODUCTION

Peptides can adopt a multitude of biologically active conformations. In particular, the β -turn motif is one of these biomolecules' most common structural features and provides a nearly 180° reverse turn.^[1-4] The β -hairpin structure, whose structural hallmark comprises two antiparallel β -strands connected by a central β -turn, is an especially interesting scaffold.^[5] It is found in a wide range of naturally occurring antimicrobial peptides (AMPs) and formed by amphiphilic sequences.^[6-9] In general, cationic amino acids mediate electrostatic attractions to the negatively charged bacterial membrane surface and the hydrophobic residues penetrate and disorganize the lipid tail region. This mode of action causes

the disruption of the physical membrane integrity and, ultimately, cell death.^[10,11]

The design of new & synthetic AMPs is of paramount interest since the emerging resistance of pathogenic microbes toward current antibiotics is a rapidly growing threat to global healthcare management.^[8,12] To overcome this limitation, the incorporation of fluorine into peptide-based antibiotics may suit as a promising approach. This element was mainly neglected in biochemical evolution^[13] but often serves as a powerful tool in medicinal chemistry for enhancing a drug's intrinsic potency and membrane permeability.^[14] The replacement of a single carbon-bonded hydrogen with a fluorine atom causes only minimal steric perturbations. However, the hydrophobic

This is an open access article under the terms of the [Creative Commons Attribution-NonCommercial-NoDerivs](https://creativecommons.org/licenses/by-nc-nd/4.0/) License, which permits use and distribution in any medium, provided the original work is properly cited, the use is non-commercial and no modifications or adaptations are made.

© 2023 The Authors. *Peptide Science* published by Wiley Periodicals LLC.

nature and polarity of an artificial amino acid are significantly affected by the number of fluorine substituents.^[15] In fact, only a few reports focusing on the selective fluorination of AMPs are available to date. In 2006, Giménez et al. described trifluoromethylated amino acids to enhance the antibacterial efficiency of cationic oligopeptides toward a few Gram-negative and Gram-positive bacterial strains.^[16] Notably, the perfluorinated amino acid L-5,5,5',5',5'-hexafluoro-leucine (HfLeu) has been extensively studied in synthetic AMPs. When incorporated into *Pexiganan*, a 22-amino acid peptide-based drug, antibiotic potencies were retained and peptide-induced hemolysis was omitted up to a concentration of 250 µg/mL.^[17] However, HfLeu-containing variants of the β-hairpin peptide *Protegrin-1* showed weaker antimicrobial activities against a diverse range of pathogenic bacteria and increased rates of hemolysis than the native AMP.^[18] Meng et al. introduced a library of HfLeu-containing *Buforin-2* and *Magainin-2* mutants and reported comprehensive improvements in antimicrobial activity but partially increased hemolysis.^[19] Further studies by Setty et al. focused on fluorine-substituted phenylalanine derivatives in AMPs and determined an overall loss in antibiotic strength upon fluorination.^[20] Summarizing these case studies, the outcome of fluorination regarding AMP potencies is controversially discussed. Similarly, divergent conclusions about the impact of fluorinated amino acids on the proteolytic stability of peptides are reported.^[21] Thus, the current state of the art in this field of research requires further systematic studies for elucidating the promising potentials of fluorinated amino acids as engineering tools in future drug development.^[22]

Our approach here was to introduce artificial amino acids with distinctive degrees of side chain fluorination into two series of amphiphilic β-hairpin peptides. We characterized their folding pattern, membrane-disrupting properties, antimicrobial, cytotoxic, and hemolytic activities. A main highlight of this report is constituted by the data set on peptide proteolysis. We provide experimental evidence that the fluorinated β-strands of each AMP are enzymatically degradable regardless of the proportions and chemical nature of the particular fluorinated side chain.

2 | EXPERIMENTAL SECTION

2.1 | General methods

¹H-, ¹³C- and ¹⁹F-NMR spectra (see Data S1) were recorded by using a JEOL ECX 400 (JEOL, Tokyo, Japan), a JEOL ECP 500 (JEOL, Tokyo, Japan) or a Bruker AVANCE III 700 (700 MHz, BRUKER, Billerica, MA, USA). Chemical shifts δ are reported in ppm with MeOH-d₄ as the internal standard. HRMS were determined on an Agilent 6220 ESI-TOF MS instrument (Agilent Technologies, Santa Clara, CA, USA). All chemicals were purchased from commercial sources (Merck, Sigma-Aldrich, VWR, Fluorochem), used without further purification, and treated according to their material safety data sheet. Chemical experiments and sample preparations were performed in ventilated fume hoods if required. All experiments were executed at settled safety precautions on laboratory safety (Freie Universität Berlin). Peptide

stock concentrations were determined via UV spectroscopy (see Data S1, Figures S33 and S34).

2.2 | Synthesis of fluorinated amino acids

The fluorinated amino acid **TfeGly** was synthesized according to protocols published by our group.^[23] The synthesis of **MfeGly** and **DfeGly** is described in the Data S1 including NMR spectra of respective amino acids. **PfpGly** was provided by Thomas Hohmann (Freie Universität Berlin) (see Data S1, Schemes S1 and S2 & Figures S1–S9).^[24]

2.3 | Synthesis and purification of peptides

All peptides were synthesized with a microwave-equipped Liberty Blue™ peptide synthesizer (CEM, Matthews, NC, USA). Detailed protocols are listed in the Data S1 (Tables S1 and S2).

All peptides were cleaved from the resin by treatment with a mixture of TFA/TIPS/H₂O (90/5/5). The crude batches were purified on a low-pressure and semi-preparative RP-HPLC system (Knauer GmbH, Berlin, Germany) with H₂O + 0.1% TFA and ACN + 0.1% TFA as HPLC solvents. Analytical HPLC was performed either on a Chromaster 600 bar DAD-system (VWR/Hitachi, Darmstadt, Germany) or a Hitachi Primaide™ DAD-system (VWR/Hitachi, Darmstadt, Germany) with both H₂O + 0.1% TFA and ACN + 0.1% TFA as HPLC solvents. All essential data (HPLC chromatograms and HRMS spectra) can be found in the Data S1 (Table S3 & Figures S10–S32).

2.4 | Sample preparation—Exchange of TFA salts

Peptide samples (about 15 mg each) were dissolved in 5 mM HCl solution (5 mL) and stirred for 1 min at rt before lyophilization. This step was repeated thrice. To remove potential leftovers of HCl, the peptide samples were subsequently dissolved in MilliQ-water (10 mL) and stirred for 1 min before lyophilization.

2.5 | CD spectroscopy

Circular dichroism experiments were performed using a Jasco J-810 spectropolarimeter using Quartz Suprasil® cuvettes (Hellma). CD spectra were recorded at 37°C from 190 to 250 nm at 0.2 nm intervals, 1 nm bandwidth, 4 s response time, and a scan speed of 100 nm min⁻¹. Baselines were subtracted from experimental data. Further experimental data can be found in the Data S1 (Figures S35 and S36).

2.6 | Carboxyfluorescein [6-FAM] leakage assay

Concentrated stocks (each 10 mg/mL) of 1-palmitoyl-2-oleoyl-sn-glycero-3-phosphocholine (POPC) and 1-palmitoyl-2-oleoyl-sn-glycero-3-[phospho-rac-(1-glycerol)] (POPG) were prepared by dissolving the

compounds in CHCl_3 . Aliquots from both stocks were mixed and CHCl_3 was evaporated. The lipid film was dried in vacuo overnight and then dissolved in 50 mM 6-carboxyfluorescein (6-FAM) in 10 mM phosphate buffer, pH 7.4. The suspension was first treated with 10 freeze-thaw cycles, then ultrasonicated at rt for 30 min, and finally rest for 1 h at rt. Untrapped 6-FAM was removed by gel filtration on PD-10 desalting columns packed with Sephadex G-25. For each sample, 25 μL of peptide solution in serial dilutions were slowly added to 25 μL of liposome solution. The final lipid concentrations were: 5 mM POPG/POPG (1:1, each 2.5 mM) or 5 mM POPC. The mixed samples were incubated for 30 min at 30°C before each measurement. 6-FAM leakage was detected by measuring the fluorescence intensity ($\lambda_{\text{ex}} = 493 \text{ nm}$ / $\lambda_{\text{em}} = 517 \text{ nm}$) with an Infinite M Nano⁺ plate reader (Tecan Deutschland GmbH, Crailsheim, Germany). 100% dye release was achieved through the addition of 5% (v/v) Triton X-100 in buffer. A negative control was constituted by measuring the FL emission of the liposome solution only containing buffer. All measurements were done in triplicates. EC_{50} values were calculated by dose-response fitting (see Data S1). Further experimental data (6-FAM leakage monitored in the case of 100% POPC) can be found in the Data S1 (Figure S37).

2.7 | Hemolytic assay

For both procedures, an approval code was not needed according to the principles of the ethical committee of our institute (Freie Universität Berlin). Further experimental data (snapshots of the treated RBC solutions) can be found in the Data S1 (Figures S42 and S43).

2.7.1 | Procedure A (XR14-series)

Purification of the erythrocytes from hRBCs containing 10% citrate phosphate dextrose was accomplished according to a published protocol by our group.^[25] In general, 1 mL pure hRBC solution was diluted with PBS buffer to a concentration of 2% hRBCs (v/v). For sample preparation, 100 μL of peptide solution in PBS buffer in serial dilutions (two-fold concentration) was added to 100 μL 2% hRBC solution. These samples were incubated at 37°C for 45 min. A [1:1] mixture of 2% (v/v) Triton X-100 and 2% hRBC solution served as a positive control and a [1:1] mixture of 2% hRBC solution with sole buffer as a negative control. After incubation, the samples were centrifuged, and the UV absorbance of the supernatants was measured at 540 nm to determine the extent of peptide-induced blood-cell hemolysis. All measurements were done in triplicates. Erythrocytes were purchased from DRK Blutspendendienst Nord-Ost Berlin.

2.7.2 | Procedure B (SAJO-series)

Purification of the erythrocytes from 8 mL whole pigs' blood was accomplished according to a published protocol by our group.^[25] In general, 1 mL pure RBC solution was diluted with PBS buffer to a concentration of 2% RBCs (v/v). The lyophilized peptides were dissolved

in PBS buffer in serial dilutions starting from a concentration of 512 $\mu\text{g}/\text{mL}$ (two-fold concentration). In a 96-well plate, 100 μL of peptide solution in PBS buffer were prepared before adding 100 μL of the 2% RBC solution. Further samples were prepared that contained only 1% RBCs in PBS buffer for serving as a negative control. Two positive controls were prepared by [1:1] mixtures of 0.2% (v/v) & 2% (v/v) Triton X-100 and 2% RBC solution. Then, the well plate was incubated at 37°C for 45 min without agitation. After that, the well plate was centrifuged and 100 μL of the supernatant was removed and added to a new 96-well plate. UV absorbance of the supernatants was measured at 540 nm to determine the extent of peptide-induced blood-cell hemolysis. All measurements were done in triplicates and **TfeGlyR14** was set as an internal control for the comparability of both approaches. The porcine blood used in this study is a surplus and was generated during clinical training (Freie Universität Berlin).

2.8 | Proteolytic digestion assay

For real-time monitoring of enzymatic digestion, peptides **AbuR14**, **TfeGlyR14**, **SAJO-2**, **SAJO-TfeGly**, and **SAJO-PfpGly** were dissolved in 10 mM phosphate buffer, pH 7.4 (125 μL) at a two-fold concentration of 200 μM and gently mixed to obtain a homogeneous mixture. After that, 125 μL of β -trypsin (0.015 μM , dissolved in 10 mM phosphate buffer, pH 7.4) was added and the samples were gently mixed for 5 s. The final reaction mixture comprised 100 μM peptide and 0.0075 μM enzyme, respectively. All samples were incubated at 30°C over a period of 3 h. Aliquots of 40 μL were taken at fixed time points and quenched with 40 μL of a solution of 5% TFA in a [1:1] water-methanol mixture containing 100 μM Ac-[2]Abz-Gly-OH as reference. Peptide degradation was monitored by HPLC analysis, and the remaining amounts of substrates were calculated by comparison to the reference signal. All experiments were performed in triplicates.

For the detection of peptide fragments derived from peptide proteolysis, all peptide samples were dissolved in 10 mM phosphate buffer, pH 7.4 (170 μL , 1 mM peptide concentration), and gently mixed to obtain a homogeneous solution. Then, 35 μL of either α -chymotrypsin or β -trypsin (both 20 μM concentration stocks in 10 mM phosphate buffer, pH 7.4) were added and the samples were gently mixed for 5 s. After that, the samples were incubated at 30°C over a period of 6 h. Aliquots of 25 μL were taken at fixed time points and quenched with 50 μL of a solution of 1% TFA in water containing 75 μM Ac-[2]Abz-Gly-OH as reference & 50 μL MeOH. Peptide degradation was monitored by HPLC analysis. For determining the digestion profile of each AMP, all detected peptide fragments were isolated and identified through HRMS analysis. All experiments were performed in triplicates.

Further experimental data can be found in the Data S1 (Tables S4 and S5 & Figures S38–S41).

2.9 | Antimicrobial susceptibility testing

Minimum inhibitory concentrations (MIC) assays were performed according to Clinical and Laboratory Standards Institute (CLSI)

recommendations in cation-adjusted Mueller-Hinton broth (Mueller-Hinton II) broth in flat-bottomed, 96-well plates (Corning, Wiesbaden, Germany) with an inoculum of 10⁵ bacteria/well. Bacteria colonies were grown on blood agar or LB agar plates overnight at 37°C, accordingly. For antimicrobial testing, these colonies were resuspended in MHII and the optical density at 600 nm was measured. The bacterial suspension was diluted right before the experiment to achieve 2×10^6 CFU/mL. From a 2.5 mg/mL peptide stock solution, a starting concentration of 2048 µg/mL was prepared. Peptide concentrations from 1024 µg/mL to 0.5 µg/mL were achieved by serial dilutions. To the wells containing 50 µL of peptide in PBS/MHII, 50 µL of bacterial suspension was added. Wells containing only MHII and bacterial suspension in MHII were prepared as a negative and positive control, respectively. The OD at 460 and 600 nm was measured at t_0 right after inoculation and after 24 h of incubation at 37°C. The resulting MIC was detected and determined as the peptide concentration where no bacterial growth could be observed after incubation.

2.10 | Cytotoxicity tests for the determination of cell viability

All cell experiments were performed according to German genetic engineering laws and German biosafety guidelines in the laboratory (safety level 1). In the case of both procedures, HeLa and A549 cells were obtained from Leibniz-Institut DSMZ—Deutsche Sammlung von Mikroorganismen und Zellkulturen GmbH.

2.10.1 | Procedure A (XR14-series)

Cell viability was determined using a CCK-8 Kit (Sigma-Aldrich). HeLa cells were cultured in DMEM and A549 in RPMI medium supplemented with 10% (v/v) FBS, 100 U/mL penicillin, and 100 µg/mL streptomycin. All cells were seeded in a 96-well plate at a density of 5×10^4 cells/mL in 90 µL DMEM/RPMI medium per well overnight at 37°C and 5% CO₂. 10 µL of peptide sample dissolved in PBS buffer were added in serial dilutions including positive (1% SDS) and negative controls (only buffer and medium) and incubated for 24 h at 37°C and 5% CO₂. For further background subtraction, wells containing only the peptide sample were used. After 24 h incubation, the CCK8 solution was added (10 µL per well) and the UV absorbance (450 nm/650 nm) was measured after about 3 h incubation. The cell viability was calculated by setting the “non-treated” control to 100% and the “non-cell” control to 0% after subtracting the background signal. For both cell lines, the experiment was performed in 3 biological replicas each containing three internal replicas.

2.10.2 | Procedure B (SAJO-series)

Cytotoxicity assays were performed using a CytoTox-ONE™ Homogenous Membrane Integrity Assay (Promega). DMEM/F-12 supplemented

with 10% v/v FBS was used for culturing the cells which were seeded at 25% confluency in 96-well well plates. These well plates were incubated at 37°C and 5% CO₂ until reaching approximately 85–90% confluency. The medium was exchanged for medium containing the AMPs in concentrations ranging from 256 µg/mL to 16 µg/mL and incubated for another 24 h. The well plates were brought to rt and 50 µL medium was removed from each well. 1 µL “Lysis Solution” was added to the wells prepared as a positive control. Subsequently, 50 µL of CytoTox-ONE™ reagent was added to each well. The well plate was shaken for 30 s and left to incubate at rt for 10 min. After incubation, 25 µL of “Stop Solution” was added. The well plate was shaken for another 10 s before the fluorescence intensity ($\lambda_{\text{ex}} = 560$ nm/ $\lambda_{\text{em}} = 590$ nm) was measured. For both cell lines, the experiment was performed in 3 biological replicas each containing three internal replicas. TfeGlyR14 was set as an internal control for the comparability of both approaches.

2.11 | Transmission electron microscopy (TEM)

E. coli (ATCC 25922) was grown in LB medium overnight and diluted to achieve an OD of 0.4 at 600 nm for all samples. To the bacterial suspension, the polyfluorinated peptide SAJO-PfpGly in PBS buffer was added to obtain bacteria/AMP mixtures containing either 2*MIC or 4*MIC. The samples were incubated at 37°C for 24 h. Additionally, control samples containing only bacteria were prepared as a negative control. Upon incubation, the samples were centrifuged at 4000 rpm for 5 min. The medium was discarded, and the pellet was resuspended in PBS buffer to remove any residual medium. After centrifuging once more and discarding the PBS wash solution, the bacterial pellets were fixed in Karnovsky fixative (7.5% glutaraldehyde, 3% paraformaldehyde) for 24 h at 5°C. Samples were washed with 0.1 M cacodylate buffer, incubated in 1% osmium tetroxide for 2 h, and washed again with cacodylate buffer. After that, the samples were dehydrated in increasing concentrations of ethanol and embedded in a mixture of epoxy resin, DDSA softener, MNA hardener, and BDMA catalyst. The resin was polymerized for 48 h at 50°C. Ultrathin sections (about 80 nm) were mounted on nickel grids and analyzed using a transmission electron microscope (TEM, JOEL, JEM-1400 Flash). TEM data can be found in the Data S1 (Figures S44 and S45).

2.12 | Thioflavin T (ThT) fluorescence spectroscopy

This experiment was performed according to a published protocol by our group.^[23] All samples were dissolved in 10 mM phosphate buffer supplemented with 20 µM Thioflavin T (ThT) (pH 7.4) and incubated for 24 h at 37°C. ThT fluorescence (FL) intensity ($\lambda_{\text{ex}} = 420$ nm, $\lambda_{\text{em}} = 485$ nm) was measured with an Infinite® M Nano⁺ plate reader (Tecan Deutschland GmbH, Crailsheim, Germany). FL values were normalized to a negative control solely containing buffer and ThT (set as FL_{int} = 1.0). The experimental data can be found in the Data S1 (Figure S46).

3 | RESULTS AND DISCUSSION

3.1 | Rational design of amphipathic peptides

We utilized the *D*-Phe-[2]Abz motif recently reported by Sarojini and co-workers.^[26–28] It is a peptidomimetic β -turn including the sterically inflexible 2-aminobenzoic acid [2]Abz. This β -amino acid has been found, for instance, in the cytotoxic cyclic tetrapeptide *Asperterrestide* A, a secondary metabolite derived from *Aspergillus terreus*.^[29,30] The turn segment consists of a linear tetrapeptide sequence [(D-Leu)^{*i*}-(D-Phe)^{*i*+1}-([2]Abz)^{*i*+2}-(D-Ala)^{*i*+3}].^[27,30] As shown in the reported crystal structure^[27] (Figure 1), the planar β -turn is stabilized by three main hydrogen bonds: (a) N–H of residue *i* with C=O of residue *i* + 3 (2.90 Å); (b) N–H of residue *i* with C=O of residue *i* + 2 (2.94 Å) and (c) an intramolecular H-bond in residue *i* + 2 (2.64 Å).^[27]

Follow-up studies by the Sarojini research group focused on the introduction of the *D*-Phe-[2]Abz motif into acyclic and cyclic AMPs.^[26,31] We decorated this β -turn unit with two Arg-rich amphipathic strands on each terminus and varied the degree of fluorination on the hydrophobic positions by iterative incorporation of either **Abu** (**AbuR14**), **MfeGly** (**MfeGlyR14**), **DfeGly** (**DfeGlyR14**) or **TfeGly** (**TfeGlyR14**) (**XR14**-series, see Table 1); the termini were capped to avoid intermolecular electrostatic repulsion. Thus, the **XR14**-series served as a systematic library for studying the beneficial effects of increasing fluorine content on AMP activity.

Besides the **XR14**-series, the peptide **SAJO-2** developed by the Sarojini research group (named peptide “2” in their work) was chosen as a reference peptide.^[26,31] Contrary to the above-described variants, this sequence possesses both terminal charges as well as a tryptophan zipper-like motif.^[32,33] Herein, investigations on the **SAJO**-scaffold aimed to fine-tune the biological activity of the control sequence with varying hydrophobicity on site-specific positions. In particular, both valine residues located at positions 2 and 13 were replaced with **Abu** (**SAJO-Abu**) or **TfeGly** (**SAJO-TfeGly**) as hydrophobic moieties. The incorporation of the pentafluoro-alkylated **PfpGly** (**SAJO-PfpGly**) constitutes, to the best of our knowledge, the first reported study of this artificial amino acid into a bioactive peptide next to its recent implementation in the β -trypsin inhibitor BPTI.^[24,34]

3.2 | Secondary structure and hydrophobicity of amphiphilic peptides

The peptide **SAJO-2** is reported to exist as a mixture of conformers in physiological conditions. Cameron et al. suggested major amounts of disordered structures according to a random coil ($\lambda_{\min} = 198$ nm) and a minor content of an ordered β -sheet pattern.^[26] Typically, the presence of type II β -turn structures can be confirmed by CD spectroscopy due to a characteristic maximum at $\lambda_{\max} = 210$ – 215 nm and negative band around $\lambda_{\min} = 225$ – 230 nm.^[35,36] We recorded CD spectra for all peptides dissolved in phosphate buffer (pH 7.4) at either 50 μ M or 500 μ M concentration (Figure 2). All peptides adopted a β -turn structure indicating no significant structural

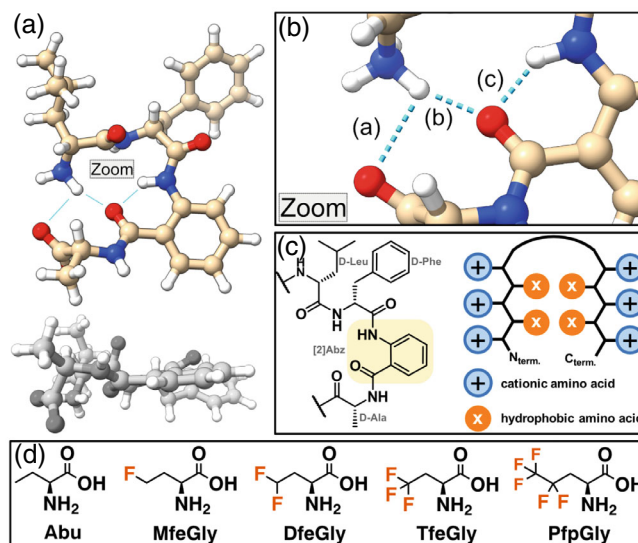


FIGURE 1 (a) Crystal structure of the linear tetrapeptide H-(D-Leu)-(D-Phe)-([2]Abz)-(D-Ala)-OH displayed from both a front view and top view (colored in gray). (b) Zoom-in view of the crystal structure with three main hydrogen bonds [(a)–(c)] maintaining this sequence in a turn-like structure (PDB Code: 6ANM). (c) Chemical structure of the *D*-Phe-[2]Abz β -turn and schematic illustration of the peptide motif (**XR14/SAJO**). [2]Abz is highlighted in yellow. (d) Chemical structures of the hydrophobic amino acids **Abu**, **MfeGly**, **DfeGly**, **TfeGly**, and **PfpGly**.

TABLE 1 Nomenclature of peptides (**XR14**-series, **SAJO**-series) and their sequences.

Peptide	Sequence
AbuR14	Ac-R- Abu -R- Abu -R-[l-f-[2]Abz-a]-R- Abu -R- Abu -R-NH ₂
MfeGlyR14	Ac-R- MfeGly -R- MfeGly -R-[l-f-[2]Abz-a]-R- MfeGly -R- MfeGly -R-NH ₂
DfeGlyR14	Ac-R- DfeGly -R- DfeGly -R-[l-f-[2]Abz-a]-R- DfeGly -R- DfeGly -R-NH ₂
TfeGlyR14	Ac-R- TfeGly -R- TfeGly -R-[l-f-[2]Abz-a]-R- TfeGly -R- TfeGly -R-NH ₂
SAJO-2	H-R-Val-R-Trp-R-[l-f-[2]Abz-a]-R-Trp-R-Val-R-OH
SAJO-Abu	H-R- Abu -R-Trp-R-[l-f-[2]Abz-a]-R-Trp-R- Abu -R-OH
SAJO-TfeGly	H-R- TfeGly -R-Trp-R-[l-f-[2]Abz-a]-R-Trp-R- TfeGly -R-OH
SAJO-PfpGly	H-R- PfpGly -R-Trp-R-[l-f-[2]Abz-a]-R-Trp-R- PfpGly -R-OH

Note: Substituted amino acids and [2]Abz are three-letter coded. Also, D-amino acids are defined by lowercase letters. Fluorinated amino acids are orange-colored.

perturbations due to side chain fluorination. Whereas a minimum at about $\lambda_{\min} = 200$ nm confirms the coexistence of random coils at 50 μ M concentration, a further increase in peptide concentration

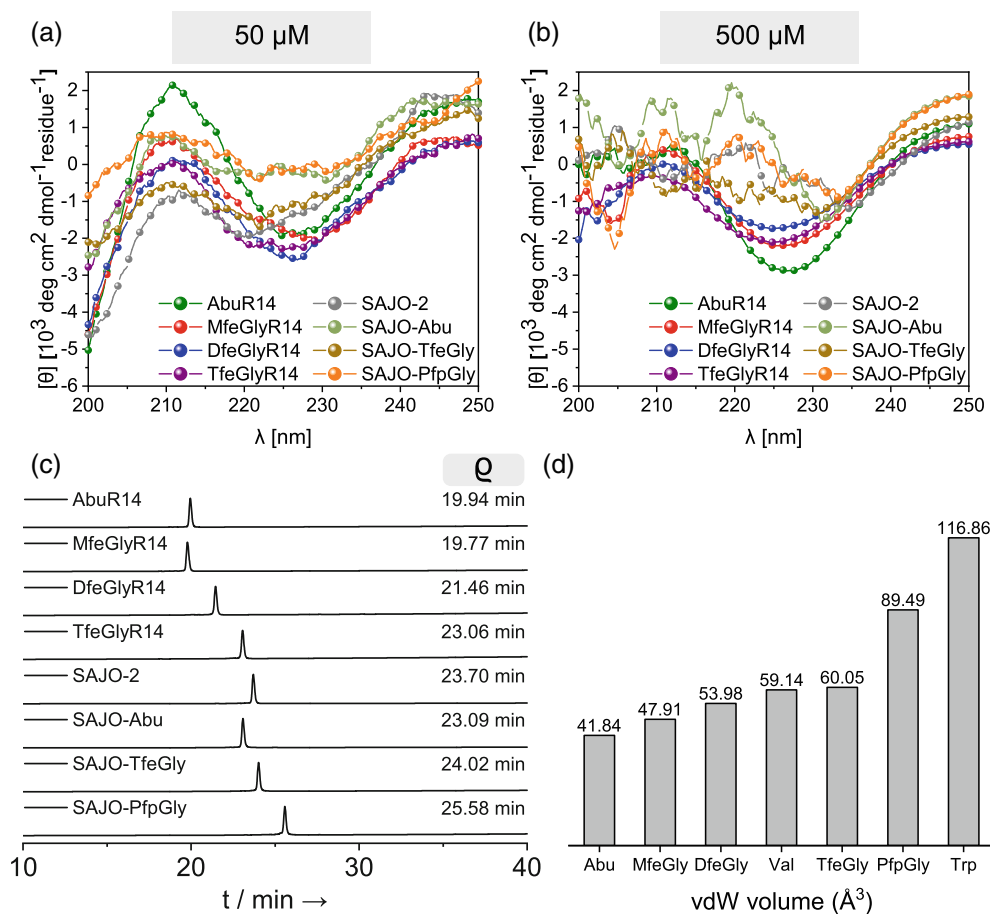


FIGURE 2 CD spectra of amphipathic peptides at (a) 50 μM and (b) 500 μM concentration dissolved in 10 mM phosphate buffer, pH 7.4, recorded at 37°C; (c) Intrinsic hydrophobicity of amphipathic peptides estimated through a RP-HPLC-based assay: The retention time ρ served as a dimension of non-polar character—HPLC conditions: CAPCELL PAK C18 MG— H_2O + 0.1% TFA/ACN + 0.1% TFA/gradient: 5% \rightarrow 70% ACN + 0.1% TFA over 40 min. (d) Calculated vdW volumes of hydrophobic amino acid side chains.

(500 μM) diminishes this course of absorption. This indicates a concentration-dependency of β -turn formation. Higher peptide concentrations led to indeterminate CD spectra for all SAJO-derivatives. This circumstance can be explained by the proximity of four aromatic amino acids within the sequences, which can produce overlapping contributions in absorption and likely result in high proportions of scattering in the CD spectra.

A RP-HPLC-based assay served to determine the hydrophobicity of each peptide in this work (Figure 2c). In addition, the van der Waals volume of each amino acid residue was calculated according to Zhao et al. (Figure 2d).^[37] The trends of enhanced lipophilic properties through fluorination determined for the XR14- and SAJO-series are in accordance with prior reports on the amino acid series Abu, MfeGly, DfeGly, and TfeGly.^[38] Increasing the fluorine content on a particular residue enhances its spatial demand as well. Monofluorination of the hydrophobic side chains (MfeGlyR14, $\rho = 19.77$ min) retains the degree of hydrophobicity compared to AbuR14 ($\rho = 19.94$ min). Further growth in fluorine content (DfeGlyR14, TfeGlyR14) enhances the intrinsic hydrophobicity significantly ($\rho = 21.46$ and 23.06 min). With regards to the SAJO-series, we determined the substitution of valine

with TfeGly to generate a peptide (SAJO-TfeGly, $\rho = 24.02$ min) with equal hydrophobicity and residual vdW volume as SAJO-2 ($\rho = 23.70$ min). SAJO-Abu ($\rho = 23.09$ min), as expected, possesses comparably less hydrophobic properties. The highest degree of hydrophobicity was found for SAJO-PfpGly ($\rho = 25.58$ min) which owns the by far most hydrophobic and largest side chain among the library of fluorinated amino acids.^[24]

3.3 | XR14-series: Evaluation of membrane-disrupting, antimicrobial, hemolytic and cytotoxic properties

We selected a 6-carboxyfluorescein (6-FAM) based leakage assay to initially probe the lytic activity of the XR14-series.^[39] When this dye is encapsulated in liposomes its fluorescence (FL) is self-quenched by intermolecular interactions. Peptide-induced disruption of the liposomes leads to a release of the dye and, therefore, can be assessed directly from the observed increase in FL intensity.^[40] The artificial liposomes were prepared in equal amounts of 1-palmitoyl-2-oleoylsn-

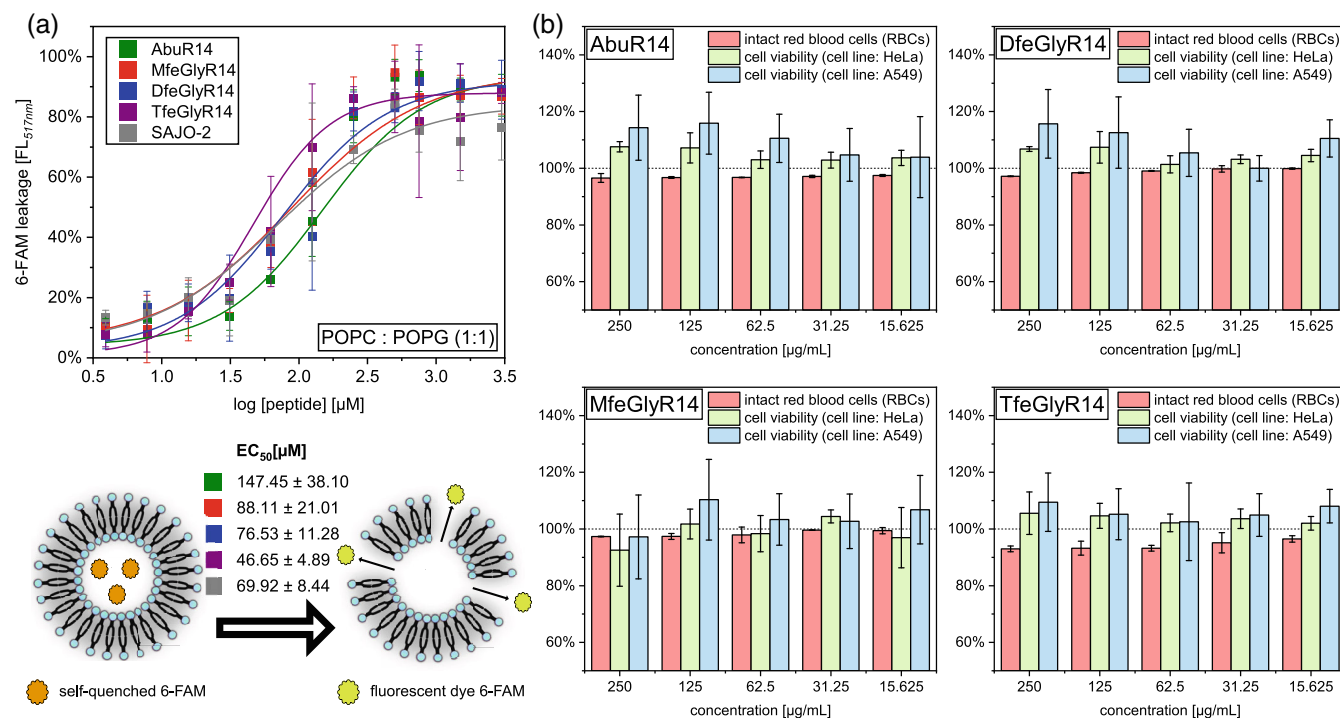


FIGURE 3 (a) Membrane permeabilization of amphipathic peptides detected via 6-FAM leaking. The dye was encapsulated in 5 mM liposome solution containing a phospholipid mixture of POPC:POPC [1:1] and its release upon the addition of peptides samples in serial dilutions after 30 min incubation (30°C) was monitored via fluorescence (FL) spectroscopy ($\lambda_{\text{ex}} = 493 \text{ nm}/\lambda_{\text{em}} = 517 \text{ nm}$). FL values were normalized to 100% dye release determined by adding 5% (v/v) Triton X-100 to the liposome solution as positive control. Dose–response curves were fitted with data sets derived from three separate experiments. The error bars show the standard deviation; (b) evaluation of peptide-induced hemolysis (incubation with 1% RBC solution) and cytotoxicity (incubation with HeLa and A549 cells) for peptides **AbuR14**, **MfeGlyR14**, **DfeGlyR14**, and **TfeGlyR14**.

glycero-3-phosphocholine (POPC) and 1-palmitoyl-2-oleoyl-sn-glycero-3-phospho-(1'-rac-glycerol) (POPG). As shown in Figure 3a, the treatment of POPC:POPG liposomes with the XR14-peptides above a threshold concentration enhances real-time detected FL intensity. Peptide-induced membrane disrupting activity was determined by calculation of EC₅₀ values. **AbuR14** possesses the weakest activity (EC₅₀ = 148 ± 39 μM) in this series and replacement with **MfeGlyR14** reduces the EC₅₀ to about 41% (88 ± 21 μM). **DfeGlyR14** (EC₅₀ = 77 ± 12 μM) revealed comparably minor changes in EC₅₀, but for **TfeGlyR14** (EC₅₀ = 47 ± 5 μM) a 3-fold optimization of membrane activity than for **AbuR14** was determined. Interestingly, this peptide possesses superior membrane activity than the reference peptide **SAJO-2** (EC₅₀ = 70 ± 9 μM). Subsequently, we checked if the multiple incorporation of hydrophobic and fluorine-containing amino acids may cause adverse effects on cell cytotoxicity and hemolysis. As shown in Figure 3b, hemolysis assays with red blood cells (RBCs) and cytotoxicity tests with two cell lines (HeLa, A549) were performed. We were pleased to determine a lack of potent hemolytic activity for all peptides up to a concentration of 250 μg/mL. Further measurements revealed peptide-induced hemolysis for the most fluorinated variant **TfeGlyR14** at minimum concentrations of 1000 μg/mL (500 μg/mL for **SAJO-2**), which is in accordance with prior observed trends of fluorine-containing AMPs (see Data S1, Figure S42).^[19,41] Furthermore, all peptides exhibited near to zero cytotoxicity up to

250 μg/mL concentration toward both cell lines. Thus, the overall proportion of fluorine in the AMPs was pivotal in the ability to permeabilize artificial phospholipid membranes without affecting the blood or human cells.

The bacterial cell envelope, however, is a complex multilayered network. The typical classification of bacterial species—Gram-positive or Gram-negative—is based on the composition of their cell walls. Gram-negative bacteria are surrounded by a thin peptidoglycan cell wall, which itself is surrounded by an outer membrane containing a variety of lipopolysaccharides. Gram-positive bacteria lack an outer membrane but are surrounded by several layers of crosslinked peptidoglycans decorated with negatively charged (lipo)teichoic acids in a thicker matrix than found in Gram-negatives.^[42] Consequently, the action mechanism of AMPs differs from the present bacterial surface. In the case of Gram-positive bacteria, an AMP must surpass the peptidoglycan barrier first before disrupting the cytoplasmic membrane. When facing Gram-negative bacteria, on the other hand, a two-step process comprising the perturbation of the outer and cytoplasmic membrane takes place.^[43,44]

Therefore, minimal inhibitory concentration (MIC) screenings for the XR14-series were performed against a variety of Gram-negative (*S. typhimurium*, *E. coli*, *P. aeruginosa*, *K. pneumoniae*) and Gram-positive (*E. faecalis*, *S. aureus*) bacteria species, but also a fungal pathogen (*C. albicans*). The MIC values are listed in Table 2 and reveal side

chain fluorination to hold a significant impact on the activity toward each pathogen but in varying magnitudes, leading to both decreased and enhanced antibiotic properties. The most fluorinated variant **TfeGlyR14** was found to be the most active AMP among the **XR14**-series but the benefits upon $-\text{CH}_3 \rightarrow -\text{CF}_3$ substitution differed. For example, we determined only a 2-fold increased potency of the fluorinated AMP when facing *S. typhimurium* (128 $\mu\text{g}/\text{mL}$) or *E. coli* (64 $\mu\text{g}/\text{mL}$). In terms of *S. aureus*, however, **AbuR14** was non-potent (≥ 1024 $\mu\text{g}/\text{mL}$) but **TfeGlyR14** was strongly active (128 $\mu\text{g}/\text{mL}$), respectively. Similar results on fluorination-enhanced potencies in the case of *S. aureus* were observed as well by the Marsh laboratory.^[17,18] These findings confirm the antimicrobial activity of this scaffold to be fine-tuned via implementation of trifluoromethylated residues (**TfeGly**) instead of a methyl group.

In terms of partially fluorinated residues, **MfeGlyR14** owns a 2- to 4-fold decreased activity than **AbuR14**, contrary to the results obtained through 6-FAM leaking assays. An interesting data set was obtained for **DfeGlyR14**: This peptide was found to be either superiorly (*S. typhimurium*, *S. aureus*) equally (*C. albicans*, *P. aeruginosa*) or less potent (*E. coli*, *E. faecalis*) than the non-fluorinated **AbuR14**. Due to its enhanced hydrophobic properties, a generous increase in antimicrobial activity for **DfeGlyR14** in comparison to **AbuR14** and **MfeGlyR14** was otherwise forecasted. We assume this circumstance to originate from fluorine-induced changes in side chain polarity. As discussed before, hydrophobicity-driven perturbations of cytosolic membranes by AMPs demand previous electrostatic attractions onto microbial cell

surfaces.^[45,46] Here, the polar character located in partially fluorinated side chains could act as a diametrical driving force against lipophilic accumulation. This interplay between fluorine-induced hydrophobicity and polarity was recently demonstrated by the Kocsch laboratory to alter supramolecular self-assembly and bioactivity.^[23,34,47] For supporting this hypothesis, the retention times of the **XR14**-peptides were plotted against recently reported water interaction energies ΔE_{int} for **Abu**, **MfeGly**, **DfeGly**, and **TfeGly** as an estimate of fluorine-induced polarity (Figure 4, left).^[23] An increase in ΔE_{int} , as given for **MfeGly**, leads to reduced hydrophobicity and, simultaneously, higher MIC values. Also, **DfeGly** possesses a much higher polarity in the side chain than **Abu** and **TfeGly**. An increasing degree of fluorination, therefore, does not automatically result in improved AMP activity. In fact, a similar trend exemplified for the antibiotic strength and ΔE_{int} indicates the impact of fluorination on antibiotic potency to be notably dependent on the side chain pattern in relation to a coaction of fluorine-enhanced polarity and hydrophobicity (see Figure 4, right).

The fungal pathogen *C. albicans* is part of the mucous flora and its yeast membrane is surrounded by a cell wall mainly composed of chitin, β -glucan, and mannoproteins.^[48] As illustrated in Figure 4, the antifungal properties of the **XR14**-series toward the pathogenic yeast follow an analogous trend of potency as determined for the bacterial species.

At last, we found all **XR14**-peptides to be non or less active toward the Gram-negative *P. aeruginosa*. We consider this circumstance to be caused by the missing Trp residues, typically present as a

TABLE 2 Antibacterial activities of peptides **AbuR14**, **MfeGlyR14**, **DfeGlyR14**, and **TfeGlyR14**.

Peptide	1*MIC [$\mu\text{g}/\text{mL}$]						
	<i>S. typhimurium</i> ATCC 14028	<i>E. coli</i> ATCC 25922	<i>E. faecalis</i> ATCC 29212	<i>S. aureus</i> ATCC 29213	<i>P. aeruginosa</i> ATCC 27853	<i>K. pneumoniae</i> ATCC 700603	<i>C. albicans</i> IMT 9655
AbuR14	256	128	512	≥ 1024	≥ 1024	≥ 1024	512
MfeGlyR14	1024	512	1024	≥ 1024	≥ 1024	≥ 1024	1024
DfeGlyR14	128	256	1024	512	≥ 1024	1024	512
TfeGlyR14	128	64	128	128	1024	512	128

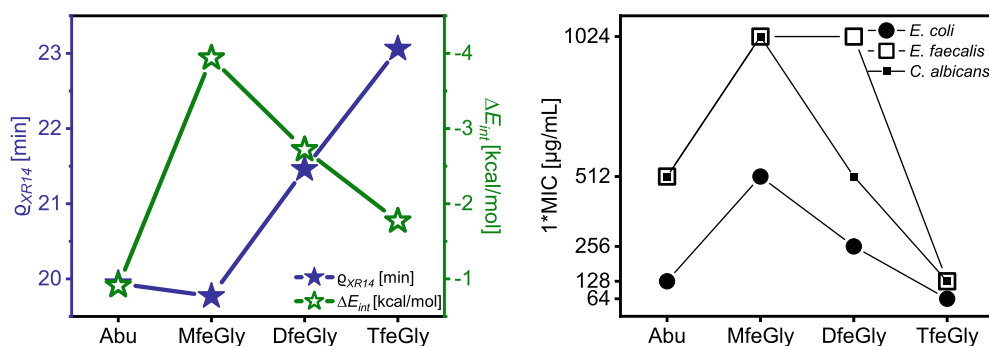


FIGURE 4 Retention times Q of **AbuR14**, **MfeGlyR14**, **DfeGlyR14**, and **TfeGlyR14** plotted against the water interaction energies ΔE_{int} calculated for **Abu**, **MfeGly**, **DfeGly**, and **TfeGly** (left). MIC values of *E. coli* (Gram-negative), *E. faecalis* (Gram-positive) and *C. albicans* (yeast fungus) plotted for each hydrophobic amino acid (**Abu**, **MfeGly**, **DfeGly**, **TfeGly**) in the **XR14**-series (right).

hydrophobic moiety in a multitude of AMPs.^[49] As reported by Shan et al., Trp-containing AMPs were particularly found to depolarize the outer and inner membrane of the bacterial cells, explaining the strong activity of tryptophane toward this bacterial species.^[50]

3.4 | SAJO-series: Evaluation of antimicrobial, hemolytic, and cytotoxic properties

The reference **SAJO-2** is reported to possess a broad spectrum of antimicrobial activity. Experimental data obtained through transmission electron microscopy (TEM) suggested this AMP to cause bacterial death by membrane lysis.^[26] MIC data of the **SAJO**-peptides (see Table 3) revealed an overall superiority in antimicrobial efficiency toward the **XR14**-series. This overall trend underlines the contribution of Trp residues to enhance membrane-disruptive properties.^[50–52]

SAJO-2 was effective against all tested organisms in concentrations ranging from 8–64 µg/mL. Similar MIC values were determined for **SAJO-TfeGly**, harmonizing with both analogous non-polar properties estimated via RP-HPLC. A loss in hydrophobicity, as probed for **SAJO-Abu**, caused a 4-fold enhanced MIC of 256 µg/mL for *E. faecalis* compared to **SAJO-2**. With regards to antifungal activities, the substitution of the hydrophobic residues led to retained MICs for *C. albicans*, very different from observations on the **XR14**-series. These results could hint at alterations in the mode of action when comparing the decrease in MIC for **AbuR14** → **TfeGlyR14**.

Most interesting MIC data were obtained for the pentafluoroalkyl-equipped peptide **SAJO-PfpGly**, which performed much better than **SAJO-TfeGly**. This polyfluorinated AMP shows the highest activity (up to 4-fold) toward all Gram-positive microbes (*S. aureus*, 16 µg/mL/*E. faecalis*, 32 µg/mL) tested in this work, as well as the Gram-negative *E. coli* (4 µg/mL). Thus, our experimental data validates the enhancement of intrinsic hydrophobicity to strengthen antimicrobial properties.

Furthermore, transmission electron microscopy (TEM) served to gain insights into the mode of action for **SAJO-PfpGly**. Incubation of *E. coli* with this AMP after 24 h was found to cause membrane pore formation, exposing a lytic and disruptive effect toward the bacterial cell wall (see Data S1, Figures S44 and S45). As illustrated in Figure 5, all **SAJO**-derivatives were tested regarding their blood cell-disrupting and cytotoxic properties. Due to the utilization of different experimental protocols (see Section 2), we set the above-discussed peptide **TfeGlyR14** as an internal control. All peptides were found in this case to be neither hemolytic nor cytotoxic. Moreover, we obtained similar

results for **TfeGlyR14** which confirmed previous studies. The only exception was found for **SAJO-PfpGly** with slightly toxic properties on the A549 cell line at the highest concentration (256 µg/mL); reducing the peptide amount, however, obviated cell cytotoxicity.

3.5 | Enzymatic degradation of (polyfluorinated) peptides

Lastly, we raised the question about the enzymatic degradability of these AMPs due to the varying degrees of side chain fluorination. The

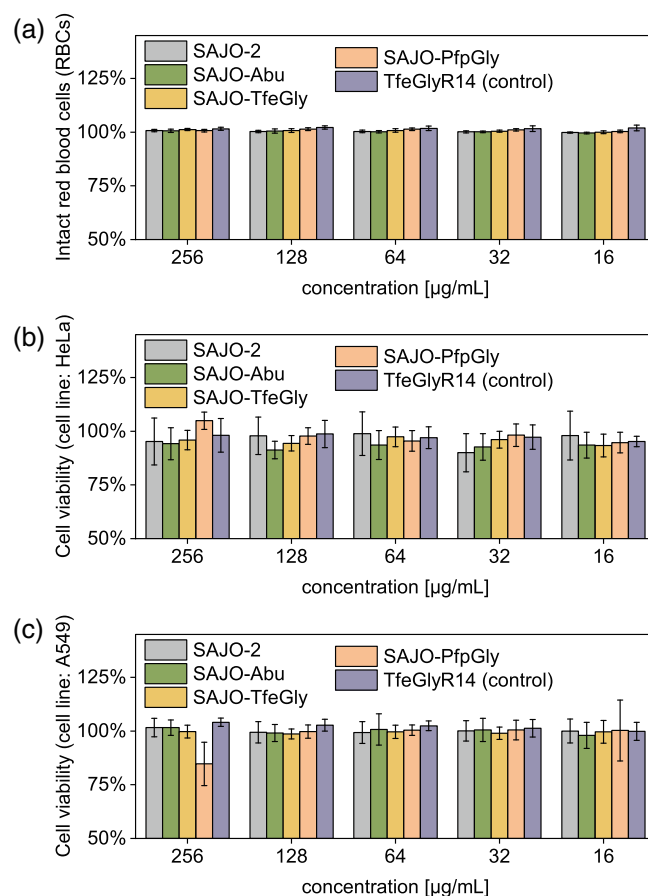


FIGURE 5 (a) Evaluation of peptide-induced hemolysis (incubation with 1% RBC solution) and cytotoxicity (incubation with (b) HeLa and (c) A549 cells) for peptides **SAJO-2**, **SAJO-Abu**, **SAJO-TfeGly**, **SAJO-PfpGly**, and **TfeGlyR14** as an internal control.

TABLE 3 Antibacterial activities of peptides **SAJO-2**, **SAJO-Abu**, **SAJO-TfeGly**, and **SAJO-PfpGly**.

Peptide	1*MIC [µg/mL]						
	<i>S. typhimurium</i> ATCC 14028	<i>E. coli</i> ATCC 25922	<i>E. faecalis</i> ATCC 29212	<i>S. aureus</i> ATCC 29213	<i>P. aeruginosa</i> ATCC 27853	<i>K. pneumoniae</i> ATCC 700603	<i>C. albicans</i> IMT 9655
SAJO-2	16	8	64	64	64	32	32
SAJO-Abu	32	16	256	64	128	64	32
SAJO-TfeGly	32	8	64	64	64	64	32
SAJO-PfpGly	16	4	32	16	64	16	32

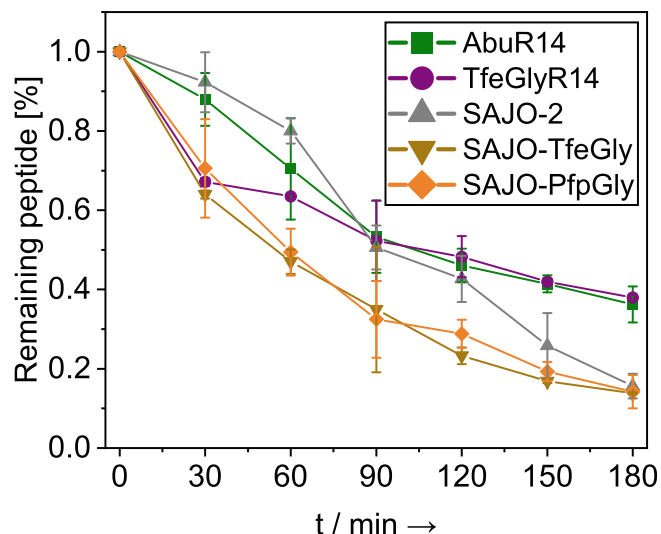


FIGURE 6 Digestion profiles of amphipathic peptides **AbuR14**, **TfeGlyR14**, **SAJO-2**, **SAJO-TfeGly**, and **SAJO-PfpGly** (all 100 μM) with β -trypsin (0.0075 μM) dissolved in 10 mM phosphate buffer, pH 7.4 and incubated at 30°C.

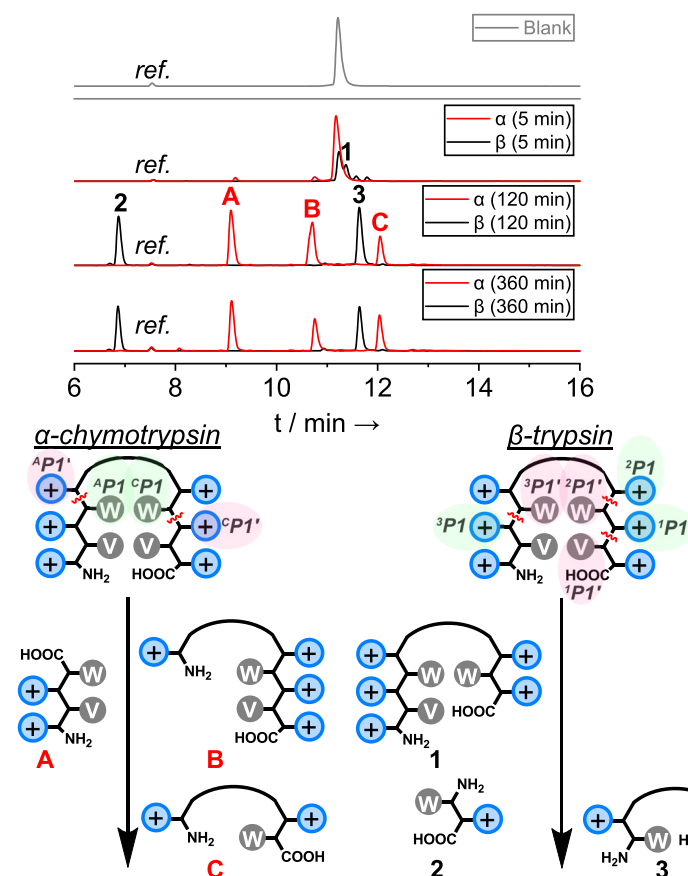
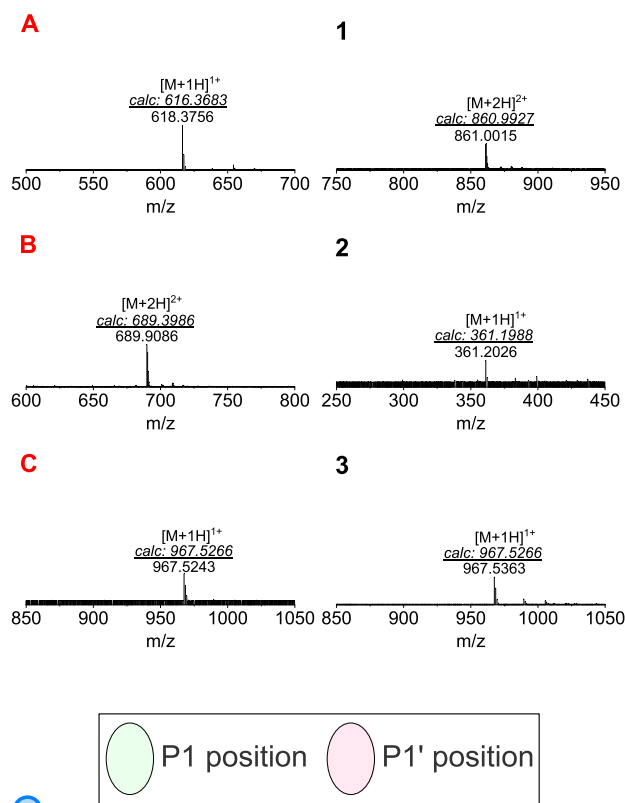


FIGURE 7 Real-time monitoring of proteolytic digestion at 5, 120 and 360 min (HPLC, DAD-280 nm) and MS-based detection and determination of peptide fragments of **SAJO-2** (1 mM stock concentration) during incubation with either α -chymotrypsin (α) or β -trypsin (β) (both 20 μM stock concentration) at 30°C. The dipeptide Ac-[2]Abz-Gly-OH was used as reference signal. The black arrows indicate the proteolysis of **SAJO-2** into the illustrated digestion fragments. Arginine residues are illustrated as blue-colored positive charges (+). Trp and Val are described with one letter abbreviations. Cleaving sites are illustrated with squiggly lines (red-colored) and defined according to *Schechter and Berger* nomenclature. Measurements were performed in triplicates.

incorporation of non-natural α -amino acid in high proportions is frequently used to alter or even eliminate primary cleaving sites, thus increasing the proteolytic stability of peptides.^[53] For example, D-amino acid substitution is well-known to protect from proteolysis by altered stereochemistry properties that prohibit sufficient enzyme-substrate binding.^[54,55] Therefore, the *D*-Phe-[2]Abz turn unit was predicted to remain persistent under enzymatic conditions.

The introduction of fluorine is extensively applied in medicinal chemistry to improve the metabolic stability of drugs.^[14,56] In the context of side chain fluorinated amino acids, however, a wide range of reports with different outcomes exists. Both cases, namely the enhanced stabilities of fluorinated peptides against proteolysis as well as rapid digestion rates due to beneficial enzyme-substrate interactions, were described.^[21,22] Various studies including our efforts identified several aspects for which fluorinated amino acids can contribute to either favored or disfavored interactions like steric bulk,^[19,57] proximity to the predominant cleavage site^[58,59] or electrostatic perturbations^[60] by a polarized side chain within an enzyme's active site.

We tested the proteolytic stability of these peptides toward the serine protease β -trypsin. This enzyme exhibits a strong S1 specificity



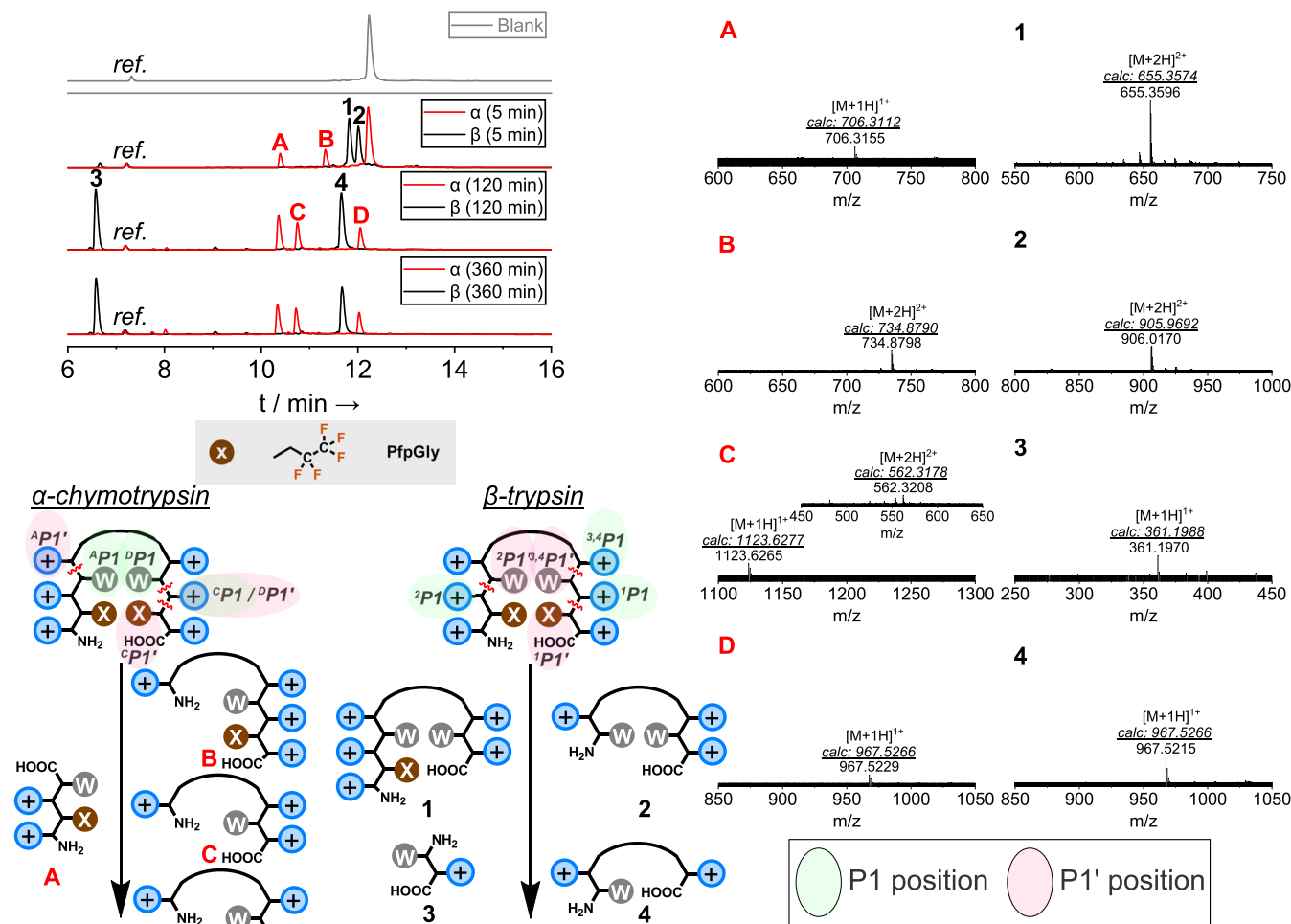


FIGURE 8 Real-time monitoring of proteolytic digestion at 5, 120 and 360 min (HPLC, DAD-280 nm) and MS-based detection and determination of peptide fragments of **SAJO-PfpGly** (1 mM stock concentration) during incubation with either α -chymotrypsin (α) or β -trypsin (β) (both 20 μ M stock concentration) at 30°C. The dipeptide Ac-[2]Abz-Gly-OH was used as reference signal. The black arrows indicate the proteolysis of **SAJO-PfpGly** into the illustrated digestion fragments. Arginine residues are illustrated as blue-colored positive charges (+). Trp is described with one letter abbreviations. Cleaving sites are illustrated with squiggly lines (red-colored) and defined according to *Schechter and Berger* nomenclature. Measurements were performed in triplicates.

(according to *Schechter and Berger* nomenclature)^[61] for Arg and Lys residues (P1 position) so that the herein-described AMPs bear multiple cleaving sites due to their amphiphilicity. In this experiment, **AbuR14**, **TfeGlyR14**, **SAJO-2**, **SAJO-TfeGly**, and **SAJO-PfpGly** were incubated at 30°C after the addition of the enzyme and their degradation profile was monitored by HPLC-analysis over a period of 3 h (Figure 6).

In fact, all peptides were found to be enzymatically degradable despite the degree of fluorination. Ultimately, the variant **SAJO-PfpGly** bearing two pentafluoroalkyl-chains was accepted as a suitable substrate by the serine protease. Real-time monitoring of peptide degradation revealed the **SAJO**-derivatives to remain in significantly lower amounts (13–15%) than **AbuR14** and **TfeGlyR14** (36–37%) after 3 h incubation. We presume this circumstance to be caused by terminal modifications of the **XR14**-derived AMPs, particularly C-terminal amidation and N-terminal acetylation. Both modifications are described to facilitate proteolytic resistance.^[62] For example, Nguyen et al. reported

greater protease stabilities of Trp- and Arg-rich peptides when both N- and C-terminal charges were capped.^[63]

Excited by this unique finding, we were engaged to determine if the presence of fluorinated amino acids also influences enzyme-substrate recognition resembled by changes in cleavage sites. For this purpose, we enhanced the concentration of the peptides (stock: 1 mM) and enzymes (stock: 20 μ M) to enable fragment detection via RP-HPLC and HRMS analysis (Figure 7 (**SAJO-2**) and Figure 8 (**SAJO-PfpGly**)). Firstly, we probed peptide digestion by the serine protease α -chymotrypsin which predominantly cleaves the amide bonds of aromatic P1 amino acids (Phe, Tyr, Trp). Also, secondary hydrolysis of bonds formed by asparagine, glutamine, methionine, glycine, histidine, and positively charged residues were reported to originate from favored P1'-S1' interactions.^[64–66] It was not surprising to observe the N-terminal aliphatic strand to be foremost cleaved (Trp: P1/Arg: P1') for both **SAJO-2** and **SAJO-PfpGly**. Interestingly, further proteolysis of digestion product "B" differed significantly for both peptides.

In the case of **SAJO-2**, this fragment remained stable during the experiment and enzyme hydrolysis was only found for the C-terminal strand between Trp (P1) and the centrally located Arg (P1') (formation of fragment “C” of **SAJO-2**) (Figure 7). In contrast, product “B” was completely consumed when both valine residues were substituted with **PfpGly** (Figure 8). We detected the release of the dipeptide fragment “PfpGly-Arg” from the C-terminal strand (formation of fragment “C” of **SAJO-PfpGly**), as well as the fragmentation up to the proteolytically stable β -turn core flanked with two Arg residues and one remaining Trp (P1) (formation of fragment “D”). It is most noteworthy that the enzyme-assisted release of the dipeptide fragment “PfpGly-Arg” confirms the fluorinated amino acid to act as a P1'-substrate for α -chymotrypsin. This finding is in accordance with earlier reports by our laboratory describing favorable side chain interactions between a few fluororous amino acids with the S1'-binding site of this serine protease.^[67,68] The branched amino acid valine (**SAJO-2**) may be unsuited as a P1'-substrate and, therefore, prevents further proteolysis. Furthermore, we examined a similar digestion profile for **SAJO-TfeGly** (see Data S1, Figure S38). Based on these results and in synergy with previous studies by Schellenberger et al., we consider the enhancement of side chain volume and fluorine-induced hydrophobicity to unleash peptide proteolysis in the case of **SAJO-PfpGly**.^[65]

When probing peptide degradation through β -trypsin, similar digestion profiles for **SAJO-2** and **SAJO-PfpGly** were again determined. The centrally located Arg residue on the C-terminal amphipathic strand acts as P1 residue leading to the formation of digestion product “1” for both peptides. This is validated by the detected cleavage of the terminal dipeptide-fragments “Val-Arg” and “PfpGly-Arg”. The P1' hydrophobic residues (Val, **PfpGly**), consequently, were accommodated within the S1' subsite. This can be explained by a broad S1' specificity of β -trypsin for aliphatic residues at P1', whereas the S2' site was reported to prefer positively charged P2' residues.^[69] In consequence, the enzyme favorably cleaves between Arg-X-Arg bonds (P1-P1'-P2', X = hydrophobic residue). Therefore, it seems that the pentafluoroalkyl-side chain of **PfpGly** neglects any interferences with the enzyme's binding pocket. After 6 h of incubation, the β -turn motif flanked with an “Arg-Trp” strand and one opposing Arg residue was found as the remaining digestion product as well as the released dipeptide fragment “Trp-Arg”. The remaining Trp residue is located at the N-terminal strand, but at the C-terminus in the case of α -chymotrypsin, which explains the slight difference in retention times depicted by HPLC analysis.

To get deeper insights into the impact of side chain fluorination on protease cleaving sites, the digestion profiles of **AbuR14**, **MfeGlyR14**, **DfeGlyR14**, and **TfeGlyR14** with both serine proteases were determined as well. All digestion profiles are placed in the Data S1 and the main cleaving sites are presented in Figure 9 for simplicity.

In the context of α -chymotrypsin, the determination of digestion products derived from the solely aliphatic strands became rather sophisticated (see *HPLC chromatograms in the Data S1, Figures S39–S41*). The lack of aromatic P1 amino acids, thus, evolved a non-specific cleavage pattern in which the hydrophobic moieties act as both P1 & P1' residues. Increasing the degree of fluorination (**DfeGly**, **TfeGly**) leads to the

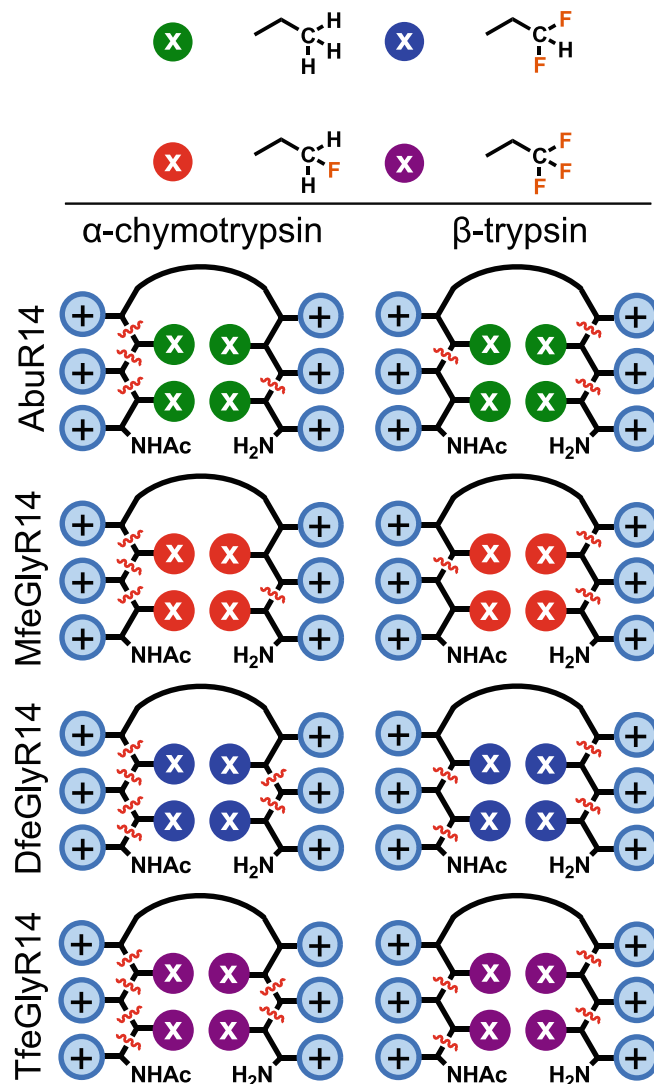


FIGURE 9 Cleavage positions observed in the enzymatic digestion of **AbuR14**, **MfeGlyR14**, **DfeGlyR14**, and **TfeGlyR14** with α -chymotrypsin and β -trypsin. Detailed digestion profiles of each peptide can be found in the Data S1. Cleaving sites are illustrated with squiggly lines (red-colored).

emergence of an Arg (P1)–fluorinated residue (P1') cleaving site on the N-terminal strand as confirmed by HPLC chromatograms & HRMS spectra. These findings further appoint higher degrees of aliphatic side chain fluorination, as present for **DfeGlyR14** and **TfeGlyR14**, to contribute to substrate recognition and peptide degradability. Similar results have been described in prior studies by Asante et al.^[67] A detailed discussion on the digestion profile of the N-terminal strands is provided in the Data S1.

On the C-terminal strand, we consider all hydrophobic residues to act as P1' residues in correlation to the centrally located Arg residue (P1). Again, the incorporation of **DfeGly** and **TfeGly** emerges a further cleaving site in which these amino acids serve as additional P1 residues. An increase in intrinsic hydrophobicity and spatial demand, consequently, acts as leverage for favored P1-S1 interactions in terms of α -chymotrypsin.

When selecting β -trypsin as an enzyme we obtained, as described for the SAJO-derivatives, comparable digestion plots. A slight difference was constituted for DfeGlyR14 and TfeGlyR14 since both substrates possess a further cleavage site between the acetylated Arg (P1) and respective hydrophobic moiety (P1') on the N-terminal strand. Similarly, an increase in fluorination exhibits an enhanced hydrophobic character and, thus, attracts the fluorinated residue into the S1' subsite of β -trypsin.

In summary, we explored and quantified a retainment of enzymatic degradability (when using α -chymotrypsin and β -trypsin) for both amphipathic motifs despite the degree of side chain fluorination. Experimentally described fluorine-triggered changes on the main cleavage sites suggest favored interactions of these non-natural derivatives with both proteases. This interesting and rarely described phenomenon^[21] is going to be further pursued in future work.

4 | CONCLUSION

In this work, we elucidated the impact of side chain fluorination on the antimicrobial activity and proteolytic stability for two series of amphipathic β -hairpin peptides. The incorporation of a wide range of unnatural & aliphatic building blocks with distinctive degrees of fluorination retained secondary structure formation and functioned as an approach to strengthen peptide hydrophobicity. MIC screenings revealed a correlation between fluorine-enhanced hydrophobicity and superior AMP activities. In this manner, the peptide SAJO-PfpGly equipped with two pentafluoro-alkylated residues was identified as the most potent AMP within this work. Simultaneously, our results may indicate a decrease in AMP activity by fluorine-induced polarity originating from the partially fluorinated side chains of MfeGly and DfeGly. All peptides presented in this work revealed zero or low values of blood cell hemolysis and cytotoxicity, which opens the door for potential therapeutical applications. Most interestingly, the implementation of fluorinated amino acids has been proven in this context to preserve peptide degradability while causing notable changes in enzyme-substrate recognition. This is supported by the identification of diverse cleaving sites for the fluorinated substrates. Our data set confirms fluorinated amino acids even with a large fluoroalkyl side chain (PfpGly) to be tolerated as substrates by α -chymotrypsin and β -trypsin; a finding that could be useful for the de novo design of artificial but enzyme-degradable peptide biomaterials. Herein described biological properties of the polyfluorinated β -hairpins highlight the tremendous opportunities which tailor-made fluorinated amino acids offer as a toolbox in modern peptide engineering to develop next-generation peptide-based antimicrobial drugs.

AUTHOR CONTRIBUTIONS

Beate Kokschi, Marcus Fulde, and Suvrat Chowdhary conceived the overall project. Beate Kokschi and Marcus Fulde provided guidance on data analysis and interpretation. Suvrat Chowdhary synthesized fluorinated amino acids and peptides, designed, and performed experiments (HPLC, CD, 6-FAM leaking, hemolysis, peptide digestion), analyzed

and interpreted data sets, and wrote the manuscript. Tim Pelzer performed MIC, toxicity, and hemolysis studies. Mareike Saathoff performed MIC studies. Elisa Quaas performed toxicity studies. Johanna Pendl performed TEM measurements.

ACKNOWLEDGMENTS

S.C. and B.K. gratefully acknowledge financial support by the Deutsche Forschungsgemeinschaft (DFG) through the collaborative research center CRC-1349 "Fluorine-Specific Interactions" project no. 387284271. We thank Dr. Anil Kumar Sahoo and Prof. Dr. Roland R. Netz for fruitful scientific discussions. We would like to acknowledge the assistance of the Core Facility BioSupraMol supported by the DFG. We thank Tiemo tom Dieck for experimental help and Pascal-Kolja Hass for TEM expertise. Finally, we thank Thomas Hohmann & Michael Dyrks for providing the fluorinated amino acid PfpGly. Open Access funding enabled and organized by Projekt DEAL.

CONFLICT OF INTEREST STATEMENT

Beate Kokschi serves as an Advisory Board member of Peptide Science and was excluded from the peer-review process and all editorial decisions related to the publication of this article. The authors declare no conflict of interest.

DATA AVAILABILITY STATEMENT

The data that support the findings of this study are available from the corresponding author (Prof. Dr. Beate Kokschi) upon reasonable request.

ORCID

Suvrat Chowdhary  <https://orcid.org/0000-0001-8669-4362>

Beate Kokschi  <https://orcid.org/0000-0002-9747-0740>

REFERENCES

- [1] R. B. Dyer, S. J. Maness, E. S. Peterson, S. Franzen, R. M. Fesinmeyer, N. H. Andersen, *Biochemistry* **2004**, 43(36), 11560.
- [2] L. Wang, N. Wang, W. Zhang, X. Cheng, Z. Yan, G. Shao, X. Wang, R. Wang, C. Fu, *Signal Transduct. Target. Ther.* **2022**, 7(1), 48.
- [3] A. G. de Brevern, *Sci. Rep.* **2016**, 6(1), 33191.
- [4] E. G. Hutchinson, J. M. Thornton, *Protein Sci.* **1994**, 3(12), 2207.
- [5] S. Fischer, M. Lamping, M. Gold, Y. Röttger, D. Brödje, R. Dodel, R. Frantz, M. A. Mraheil, T. Chakraborty, A. Geyer, *Bioorg. Med. Chem.* **2017**, 25(2), 603.
- [6] S.-n. Nishimura, K. Nishida, M. Tanaka, *Chem. Commun.* **2022**, 58(4), 505.
- [7] G. Wang, X. Li, Z. Wang, *Nucleic Acids Res.* **2016**, 44(D1), D1087.
- [8] Y. Huan, Q. Kong, H. Mou, H. Yi, *Front. Microbiol.* **2020**, 11(2559), 1-21.
- [9] J.-P. S. Powers, R. E. W. Hancock, *Peptides* **2003**, 24(11), 1681.
- [10] R. Kundu, *ChemMedChem* **2020**, 15(20), 1887.
- [11] J. A. Killian, G. von Heijne, *Trends Biochem. Sci.* **2000**, 25(9), 429.
- [12] K. Lewis, *Nat. Rev. Drug Discov.* **2013**, 12(5), 371.
- [13] N. Budisa, V. Kubyschkin, D. Schulze-Makuch, *Life* **2014**, 4(3), 374.
- [14] E. P. Gillis, K. J. Eastman, M. D. Hill, D. J. Donnelly, N. A. Meanwell, *J. Med. Chem.* **2015**, 58(21), 8315.
- [15] M. Salwiczek, E. K. Nyakatura, U. I. M. Gerling, S. Ye, B. Kokschi, *Chem. Soc. Rev.* **2012**, 41(6), 2135.

- [16] D. Giménez, C. Andreu, M. I. d. Olmo, T. Varea, D. Diaz, G. Asensio, *Bioorg. Med. Chem.* **2006**, *14*(20), 6971.
- [17] L. M. Gottler, H. Y. Lee, C. E. Shelburne, A. Ramamoorthy, E. N. Marsh, *ChemBioChem* **2008**, *9*(3), 370.
- [18] L. M. Gottler, R. de la Salud Bea, C. E. Shelburne, A. Ramamoorthy, E. N. G. Marsh, *Biochemistry* **2008**, *47*(35), 9243.
- [19] H. Meng, K. Kumar, *J. Am. Chem. Soc.* **2007**, *129*(50), 15615.
- [20] S. C. Setty, S. Horam, M. Pasupuleti, W. Haq, *Int. J. Pept. Res. Ther.* **2017**, *23*(2), 213.
- [21] S. Huhmann, B. Koksich, *Eur. J. Org. Chem.* **2018**, 2018(27–28), 3667.
- [22] Z. Lai, X. Yuan, H. Chen, Y. Zhu, N. Dong, A. Shan, *Biotechnol. Adv.* **2022**, *59*, 107962.
- [23] S. Chowdhary, R. F. Schmidt, A. K. Sahoo, T. tom Dieck, T. Hohmann, B. Schade, K. Brademann-Jock, A. F. Thünemann, R. R. Netz, M. Grzdzinski, B. Koksich, *Nanoscale* **2022**, *14*(28), 10176.
- [24] T. Hohmann, M. Dyrks, S. Chowdhary, M. Weber, D. Nguyen, J. Moschner, B. Koksich, *J. Org. Chem.* **2022**, *87*(16), 10592.
- [25] C. K. Thota, A. A. Berger, B. Harms, M. Seidel, C. Böttcher, H. von Berlepsch, C. Xie, R. Süßmuth, C. Roth, B. Koksich, *Pept. Sci.* **2020**, *112*(1), e24130.
- [26] A. J. Cameron, K. G. Varnava, P. J. B. Edwards, E. Harjes, V. Sarojini, *J. Pept. Sci.* **2018**, *24*(8–9), e3094.
- [27] A. J. Cameron, C. J. Squire, P. J. B. Edwards, E. Harjes, V. Sarojini, *Chem. Asian J.* **2017**, *12*(24), 3195.
- [28] A. J. Cameron, P. J. B. Edwards, E. Harjes, V. Sarojini, *J. Med. Chem.* **2017**, *60*(23), 9565.
- [29] F. He, J. Bao, X. Y. Zhang, Z. C. Tu, Y. M. Shi, S. H. Qi, *J. Nat. Prod.* **2013**, *76*(6), 1182.
- [30] S. S. Kale, G. Priya, A. S. Kotmale, R. L. Gawade, V. G. Puranik, P. R. Rajamohanam, G. J. Sanjayan, *Chem. Commun.* **2013**, *49*(22), 2222.
- [31] K. G. Varnava, P. J. B. Edwards, A. J. Cameron, E. Harjes, V. Sarojini, *J. Pept. Sci.* **2020**, *27*, e3291.
- [32] T. Podewin, M. S. Rampp, I. Turkanovic, K. L. Karaghiosoff, W. Zinth, A. Hoffmann-Röder, *Chem. Commun.* **2015**, *51*(19), 4001.
- [33] A. G. Cochran, N. J. Skelton, M. A. Starovasnik, *Proc. Natl. Acad. Sci. U. S. A.* **2001**, *98*(10), 5578.
- [34] J. Leppkes, N. Dimos, B. Loll, T. Hohmann, M. Dyrks, A. Wieseke, B. G. Keller, B. Koksich, *RSC Chem. Biol.* **2022**, *3*(6), 773.
- [35] T. L. Gururaja, S. Narasimhamurthy, D. G. Payan, D. C. Anderson, *Chem. Biol.* **2000**, *7*(7), 515.
- [36] S. Brahm, J. Brahm, *J. Mol. Biol.* **1980**, *138*(2), 149.
- [37] Y. H. Zhao, M. H. Abraham, A. M. Zissimos, *J. Org. Chem.* **2003**, *68*(19), 7368.
- [38] U. I. M. Gerling, M. Salwiczek, C. D. Cadicamo, H. Erdbrink, C. Czekelius, S. L. Grage, P. Wadhvani, A. S. Ulrich, M. Behrends, G. Haufe, B. Koksich, *Chem. Sci.* **2014**, *5*(2), 819.
- [39] T. Vagt, O. Zschörnig, D. Huster, B. Koksich, *ChemPhysChem* **2006**, *7*(6), 1361.
- [40] J. N. Weinstein, R. Blumenthal, R. D. Klausner, *Methods Enzymol.* **1986**, *128*, 657.
- [41] B. C. Buer, E. N. G. Marsh, *Protein Sci.* **2012**, *21*(4), 453.
- [42] T. J. Silhavy, D. Kahne, S. Walker, *Cold Spring Harbor Perspect. Biol.* **2010**, *2*(5), a000414.
- [43] H. Nikaïdo, *Microbiol. Mol. Biol. Rev.* **2003**, *67*(4), 593.
- [44] F. P. Tally, M. F. DeBruin, *J. Antimicrob. Chemother.* **2000**, *46*(4), 523.
- [45] N. Malanovic, K. Lohner, *Biochim. Biophys. Acta (BBA) Biomembr.* **2016**, *1858*(5), 936.
- [46] J. Li, J.-J. Koh, S. Liu, R. Lakshminarayanan, C. S. Verma, R. W. Beuerman, *Front. Neurosci.* **2017**, *11*, 1–18.
- [47] S. Chowdhary, J. Moschner, D. J. Mikolajczak, M. Becker, A. F. Thünemann, C. Kästner, D. Klemczak, A.-K. Stegemann, C. Böttcher, P. Metrangolo, R. R. Netz, B. Koksich, *ChemBioChem* **2020**, *21*(24), 3544.
- [48] R. Garcia-Rubio, H. C. de Oliveira, J. Rivera, N. Trevijano-Contador, *Front. Microbiol.* **2020**, *10*, 1–13.
- [49] S. Clark, T. A. Jowitt, L. K. Harris, C. G. Knight, C. B. Dobson, *Commun. Biol.* **2021**, *4*(1), 605.
- [50] X. Zhu, Z. Ma, J. Wang, S. Chou, A. Shan, *PLoS One* **2014**, *9*(12), e114605.
- [51] H. Khandelia, Y. N. Kaznessis, *J. Phys. Chem. B* **2007**, *111*(1), 242.
- [52] X. Bi, C. Wang, W. Dong, W. Zhu, D. Shang, *J. Antibiot.* **2014**, *67*(5), 361.
- [53] Z. Feng, B. Xu, *Biomol. Concepts* **2016**, *7*(3), 179.
- [54] Y. P. Di, Q. Lin, C. Chen, R. C. Montelaro, Y. Doi, B. Deslouches, *Sci. Adv.* **2020**, *6*(18), eaay6817.
- [55] T. Manabe, K. Kawasaki, *Sci. Rep.* **2017**, *7*(1), 43384.
- [56] I. Ojima, *J. Org. Chem.* **2013**, *78*(13), 6358.
- [57] H. Meng, S. T. Krishnaji, M. Beinborn, K. Kumar, *J. Med. Chem.* **2008**, *51*(22), 7303.
- [58] V. Asante, J. Mortier, H. Schlüter, B. Koksich, *Bioorg. Med. Chem.* **2013**, *21*(12), 3542.
- [59] S. Huhmann, A. K. Stegemann, K. Folmert, D. Klemczak, J. Moschner, M. Kube, B. Koksich, *Beilstein J. Org. Chem.* **2017**, *13*, 2869.
- [60] B. Koksich, N. Sewald, H.-J. Hofmann, K. Burger, H.-D. Jakubke, *J. Pept. Sci.* **1997**, *3*(3), 157.
- [61] I. Schechter, A. Berger, *Biochem. Biophys. Res. Commun.* **1968**, *32*(5), 898.
- [62] D. Li, Y. Yang, R. Li, L. Huang, Z. Wang, Q. Deng, S. Dong, *J. Pept. Sci.* **2021**, *27*(9), e3337.
- [63] L. T. Nguyen, J. K. Chau, N. A. Perry, L. de Boer, S. A. J. Zaat, H. J. Vogel, *PLoS One* **2010**, *5*(9), e12684.
- [64] R. L. Hill, in *Advances in Protein Chemistry*, Vol. 20 (Eds: C. B. Anfinsen, M. L. Anson, J. T. Edsall, F. M. Richards), Academic Press, **1965**, p. 37. Cambridge, Massachusetts.
- [65] V. Schellenberger, U. Schellenberger, Y. V. Mitin, H. D. Jakubke, *Eur. J. Biochem.* **1990**, *187*(1), 163.
- [66] L. Hedstrom, *Chem. Rev.* **2002**, *102*(12), 4501.
- [67] V. Asante, J. Mortier, G. Wolber, B. Koksich, *Amino Acids* **2014**, *46*(12), 2733.
- [68] S. Huhmann, E. K. Nyakatura, H. Erdbrink, U. I. M. Gerling, C. Czekelius, B. Koksich, *J. Fluorine Chem.* **2015**, *175*, 32.
- [69] T. Kurth, S. Grahn, M. Thormann, D. Ullmann, H.-J. Hofmann, H.-D. Jakubke, L. Hedstrom, *Biochemistry* **1998**, *37*(33), 11434.

SUPPORTING INFORMATION

Additional supporting information can be found online in the Supporting Information section at the end of this article.

How to cite this article: S. Chowdhary, T. Pelzer, M. Saathoff, E. Quaas, J. Pendl, M. Fulde, B. Koksich, *Pept. Sci.* **2023**, *115*(3), e24306. <https://doi.org/10.1002/pep2.24306>